九州大学大学院
システム情報科学紀要
第 17 巻　第 1 号　平成 24 年 5 月

Research Reports on Information Science and
Electrical Engineering of Kyushu University
Vol.17, No.1, May 2012

Global Localization for a Mobile Robot Using Laser Reflectance and Particle Filter

DongXiang ZHANG* and Ryo KURAZUME**

(Received April 16, 2012)

Abstract: Global localization is a fundamental requirement for a mobile robot. Map-based global localization is a popular technique and gives a precise position by comparing a provided geometric map and current sensory data. However, it is quite time-consuming if 3D range data is processed for 6D global localization. On the other hand, appearance-based global localization using a captured image and recorded images is simple and suitable for real-time processing. However, this technique does not work in the dark or in an environment in which the lighting conditions change remarkably. To cope with these problems, we have proposed a two-step strategy which combines map-based global localization and appearance-based global localization. Firstly, several candidate positions are selected according to an appearance-based technique, and then the optimum position is determined by a map-based technique. Instead of camera images, we use reflectance images, which are captured by a laser range finder as a by-product of range sensing. In this paper, a new technique based on this global localization technique is proposed by combining the two step algorithm and a sampling-based approach. To cope with the odometry data, a particle filter is adopted for tracking robot positions. The effectiveness of the proposed technique is demonstrated through experiments in real environments.

Keywords: Global localization, Mobile robot, Laser range finder, Reflectivity, Bag of features, Particle filter

1. Introduction

In numerous practical applications, the external environment around a robot is unpredictable, unstructured, and uncontrolled. For example, in an area that has been struck by a strong earthquake or by a mine disaster, previously navigable areas may be blocked by heaps of rubble or collapsed walls, and the geometric structure will differ from the original structure. In order for a robot to efficiently accomplish search and rescue tasks in this type of unknown and unpredictable environment, accurate map creation and global localization are fundamental requirements.

A number of global localization techniques have been proposed[11]. Appearance-based global localization is simple and suitable for real-time processing. Many camera images are recorded under natural light or indoor illumination in the environment, and global localization is performed by finding the best match using a newly-captured image and stored images[13],[14]. However, appearance-based global positioning encounters a critical problem in dark environments or in environments in which the lighting condition changes dramatically.

On the contrary, map-based global localization, which determines the best position at which the observed geometric features from sensory data match those in the provided geometric map, is a standard and reliable technique since this method is applicable for various sensors and environments[1],[8]. From the point of view of accuracy, comparison of 3D range data captured by a range sensor and a pre-constructed 3D map is preferable because this will enable precise 6D (position and attitude) global localization. However, the comparison with large 3D data is quite time-consuming.

To cope with this problem, we have proposed a two-step strategy that combines map-based global localization and appearance-based global localization and verified its efficiency in outdoor environment in 21). Instead of camera images, which are used for the appearance-based global localization, we used reflectance images, which are captured by a laser range finder as a byproduct of range sensing. As a result of the characteristics of the reflectance image, which is not subject to significant variation of the external illumination conditions, the proposed technique is useful even in the dark or in an environment under severe lighting conditions. Furthermore, fast and precise localization can be performed by comparing a few 3D range images, which are selected based on the similarity of the reflectance images. However, since this method relies on the similarity between newly-captured and stored reflectance images, the performance is deteriorated under perceptual aliasing conditions such as in a corridor or in a mine.

*Department of Advanced Information Technology, Graduate Student
**Department of Advanced Information Technology

Particle filter localization is an effective method for robotic application by Bayesian inference. The robustness for robot localization and mapping in a scene with few or similar features such as a corridor[16),19)], a mine[7)] and so on has been demonstrated. Therefore, we propose a new global localization technique which combines the proposed two-step strategy and the particle filter. We will demonstrate that our method can achieve robust and precise robot localization in environments with strong perceptual aliasing even under severe variation of external illumination conditions.

The remainder of this paper is organized as follows. After a brief introduction of related research in Section 2, Section 3 introduces the cooperative positioning system on which the proposed method is based. The proposed two-step strategy combined with particle filter is described in detail in Sections 4, and experimental results are presented in Section 6.

2. Related research

In the robotics community, appearance-based localization using camera images which is very close to the sensing way of human being has achieved great success. The BoF technique is successfully applied to the appearance-based SLAM problem. It first extracts local features of an image and then constructs a histogram using the extracted local features as a representation of the global features. In 2), the loop closure detection, which is a problem to find a location where the robot previously visited, was solved by the BoF technique in a probabilistic manner. However, these methods assume that the illumination condition does not change so severely. Therefore, the travel distance of the robot must be short enough so that the lighting condition will not change drastically. In another study, the experimental results were not evaluated explicitly under significant changes in illumination[3)]. These methods will fail in the dark or in environments in which the lighting is dramatically changed.

When range is measured by a laser range finder, the reflectivity, which indicates the strength of the reflected laser, can be obtained as a byproduct of range data. Note that all of the pixels in the range image have corresponding reflectance values. In other words, the range image and the reflectance image are precisely and fundamentally aligned. In addition, since the reflectance image is not subject to any extreme variations in the external illumination conditions, stable reflectance images can be obtained even at night.

Kara et al.[4)] utilizes reflection intensity from a 1D laser range finder for localization in 2D space. On the other hand, our technique utilizes 2D reflectance images obtained by a 3D laser range finder for 3D localization. The proposed technique uses a panoramic reflectance image instead of a regular camera image. By applying the BoF technique for a reflectance image that corresponds to 3D range data, the global localization using 3D range data and 2D images is achieved efficiently. Levinson et al.[8)] utilize 2D infrared reflectivity map to achieve a real-time autonomous vehicle navigation. Firstly they created a spatial grid map with infrared remittance values in a probabilistic manner using SLAM technology and determined the vehicle position on-line with the 2D infrared reflectivity map and a GPS/IMU system.

Particle filter (Monte carlo localization) is a useful probabilistic inference algorithm[12)]. In particle filter algorithm, the probabilities of Bayesian inference are represented as many particles. Particle filter has been applied in many successful robot systems. Wolf et al.[16)] integrates Monte carlo localization (MCL) with an image retrieval system. Andreasson et al.[17)] integrates Monte carlo localization with a panoramic imaging system. Zingaretti et al.[19)] compares two different MCL systems, one using SIFT-based vision system and the other using sonar sensing system, then it combines these two system to get better localization under perceptual aliasing conditions.

The algorithm framework of the proposed technique is similar to that described in 16) and 17) which weight the particles according to the results of the image retrieval process. However, since these techniques[16)17)] depend on conventional camera images, it apparently would fail under severe variation of illumination.

3. 3D global map with reflectivity

3.1 Three-dimensional global map

The process of mapping the entire field is displayed in **Fig. 1**. This process is based on a precise localization technique using parent-child robots named Cooperative Positioning System (CPS). The detail of CPS is shown in appendix.

In each location, the parent robot collects a local 3D map and its measurement position based on the relative observation between the parent and child robots. Eventually, all of the local 3D maps are aligned into a global 3D map using the measurement position information. Additional details about CPS-based simultaneous localization and mapping (CPS-SLAM) can be found in 5).

3.2 Reflectance images

As mentioned above, reflectance images are captured

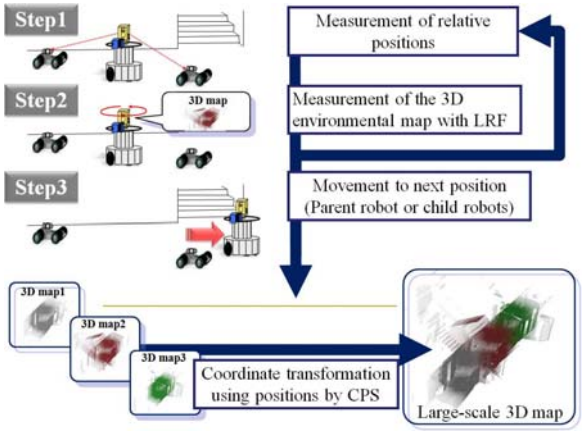

Fig. 1 Construction of a large-scale 3D map by the CPS.

as a byproduct of range sensing. Examples of a reflectance image and its corresponding camera image taken in the night are shown in **Fig. 2**. Some examples of the 3D data and reflectance images acquired by CPS-VI are shown in **Fig. 3** and **Fig. 4**. Note that each reflectance image contains the position information for the location at which the image was captured. These images are used for appearance-based global localization in the proposed two-step strategy.

Fig. 2 Reflectance image and camera image in corridor.

Fig. 3 Two sideviews of local 3D map.

3.3 Image retrieval using the BoF technique

When the global 3D map of the target field is constructed, a Kd-tree structure storing BoF representations of reflectance images is also constructed at the same time. Reflectance images are represented as histograms of occurrence of the visual words in an image. SIFT and SURF[20)18)] are well used in appearance-based robot localization for extracting features. First, regions in feature space are mapped to visual words by clustering all SURF or SIFT features extracted from recorded

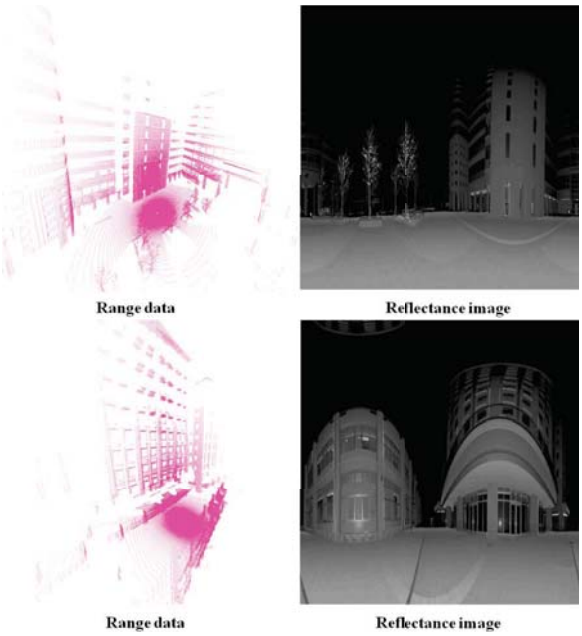

Fig. 4 Reflectance and range images in outdoor.

images into representative words using k-means clustering, and the words are stored using a Kd-tree structure. Using these words as the x-axis, we quantize each feature in a reflectance image to its approximate nearest word by searching the Kd-tree, and all of the recorded reflectance images are represented as statistics of words (histograms). Finally, the histograms of all recorded images are stored using a Kd-tree structure. A newly-captured image is also represented as a histogram, and M images that best match the newly-captured image are retrieved by quantizing the histogram to its nearest M histograms. These M candidates are used as the observation model of particle filter.

4. Two-step strategy

This section presents the two-step strategy for precise localization using a 3D map. First, we need to create a global map as a training dataset. As explained in Section 3, the CPS robots move in the environment and construct a 3D global map. At the same time, the parent robot collects reflectance images at each measurement position. Then, all of reflectance images are represented using the BoF technique, and a training dataset is created. Finally, the dataset of all of the BoF representations is stored in a Kd-tree, which is efficient for information retrieval.

For global localization, a new robot that is equipped with a 3D range sensor, such as CPS-VI, collects local 3D data and 2D reflectance images (test data). In the first step, we retrieve M initial location candidates by comparing stored reflectance images (training dataset)

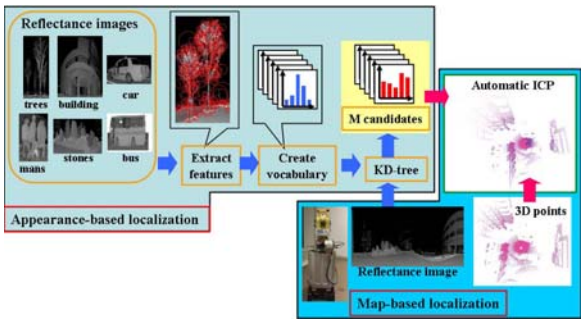

Fig. 5 Combination of appearance-based localization and map-based localization.

and captured reflectance images (test data) using the BoF technique and a Kd-tree. Next, we apply particle filter for extracting a correct initial location candidate from these M candidates. By using the particle filter, particles converge to few locations, and false initial locations are excluded. So only a few initial candidates are left for the next precise localization. We then apply a 3D geometric constraint in order to extract true feature pairs and run automatic ICP in the second step. As a result of the first step, fast and precise localization can be performed in the second step by comparing only one 3D range images, which is selected based on the similarity of the reflectance images and probabilistic inference in the first step.

The entire process is shown in **Fig. 5**. Generally speaking, although ICP gives precise alignment results, it is quite time-consuming. However, since only a small number (M) of reference dataset are selected by the first step based on the similarity of the reflectance images, fast and precise localization can be performed using automatic ICP in the second step.

We hereinafter denote $Train\_i.ref$ and $Train\_i.pts$ as the i^{th} reflectance image and the local 3D map, respectively, in the training dataset, and $Test\_j.ref$ and $Test\_j.pts$ as the j^{th} reflectance image and the local 3D map, respectively, in the test dataset. In the following, the proposed two-step strategy is described in detail.

4.1 First step: image retrieval and particle filter

4.1.1 Image retrieval by BoF using 2D reflectance images

All $Test\_j.ref$ are converted into BoF representations, and the M best matches are searched in the Kd-tree that was constructed from the training dataset. The M $Train\_i.ref$ and $Train\_i.pts$ are then selected as M candidates for the position of the robot in the 3D global map.

4.1.2 Particle filter

When the reflectance images are collected, the positions are also recorded by CPS, so a topological graph in which each node is represented by a reflectance image is created. By the results of image retrieval, M candidates location in the topological graph are used for the observed data of particle filter. The particles will converge to one of M candidates. The details are described at Section 5.

4.2 Second step: precise measurement by automatic ICP using 3D data

With the position of particle after convergence, automatic ICP[9)10)] which consists of two processes is applied. However, before applying automatic ICP, 3D geometric constraints are used to remove outliers. In some cases, the number of false outliers is large than true inliers, therefore we have proposed a two-step voting algorithm based on 3D geometric constraints to remove outliers efficiently in 21). The process of automatic ICP is as follows:

(1) Rough alignment with RANSAC
   (a) Find the corresponding features between $Test\_j.ref$ and $Train\_i.ref$.
   (b) Get the 3D coordinates of corresponding features using $Test\_j.pts$ and $Train\_i.pts$, which correspond to $Test\_j.ref$ and $Train\_i.ref$, respectively.
   (c) Remove outliers by two-step voting algorithm.
   (d) 3D transformation between $Test\_j.pts$ and $Train\_i.pts$ is estimated by RANSAC.
   (e) Align $Test\_j.pts$ to $Train\_i.pts$.
(2) Precise alignment with ICP
   (a) Run ICP[9)] using $Test\_j.pts$ and $Train\_i.pts$, which are already roughly aligned.

5. SIR particle filter

Sequential Importance Resampling (SIR) particle filter is a kind of Bayesian filtering techniques which estimate the belief recursively. The key idea of particle filter is representing the probabilistic belief $p(X_t|o,a)$ of robot's location by a set of weighted particles. The probability of current state X_t given a history of action and observation (abbreviated as *a and o*, respectively) is approximated as:

$$S_t = \{x_t^{(i)},\ \pi_t^{(i)}\},\ i = 1...N \quad (1)$$

Each particle $x_t^{(i)}$ represents a hypothesized state with a non-negative numerical weight $\pi_t^{(i)}$. The alternating three main steps of SIR particle filter are as follows:

(1) Generate a new set of particles S_{t+1} by resampling from old particle set S_t according to particle weights

$\pi_t^{(i)}, i = 1...N$

(2) Predict the next state of new particle set based on the motion model with additional Gaussian noise.

(3) Calculate the new weights of new particles, this is done by integrating the observation model into the weight of each particle.

The details how particle filter is applied in our robot system is described as follows:

5.1 Motion model

When a robot is visiting the target environments, all particle variables $x_t^{(i)} = (x, y, \phi)_t^{(i)}$ where (x, y) is the robot position in 2D grid map and ϕ is the orientation, are updated according to the movement between adjacent measurement positions which are obtained by odometry or other local localization techniques such as CPS. Meanwhile the particle variables are updated with small random values drawn from a normal distribution, using a standard deviation of var_yaw for the rotation and a standard deviation of var_x and var_y for the translation.

5.2 Observation model

In each location, with the current scanned reflectance image, M candidate positions $o_t^{(j)}$ from training dataset of reflectance images are searched out by Kd-tree. In M candidates only the one whose collecting location is closest to the current particle is used for calculating its weight. From the automatic ICP, the rotation angle ϕ can be calculated correctly, it doesn't need to be used for calculating weights. The weighting function is defined as:

$$f_w(d) = exp(-\frac{d^2}{\delta^2}) \tag{2}$$

d is the minimum Euclidean distance between $x_t^{(i)}$ and $o_t^{(j)}, j = 1...M$,

$$d = \min_{j=1}^{M} ||x_t^{(i)} - o_t^{(j)}|| \tag{3}$$

5.3 Location estimation

The particles will converge to a location at each loop in the process of SIR. The convergent particles' location is the roughly estimated robot's position. With the current convergent location, the reflectance image whose location is closest to it is selected. This means that two corresponding reflectance images are found: one is the current reflectance image, and another is the searched reflectance image from training dataset. With this two reflectance images and their corresponding 3D point data, the robot's location can be precisely estimated by automatic ICP.

6. Experiment and Results

The experiment is conducted in an environment with strong perceptual aliasing in order to verify the performance of the proposed two-step strategy. The 2D map for the experiment is shown in **Fig. 6** which is created in a corridor. There are many similar scenes in this path. Two pairs of similar scenes are also shown in **Fig. 6**, examples of reflectance image and corresponding 3D points data have been shown in **Fig. 2** and **Fig. 3**. In this experiment, the size of reflectance images is 590×2264 pixels. The CPS-VI robots move and stop at 72 different locations in the experimental area in **Fig. 6**, i.e. 72 data ($Train\_i.ref$ and $Train\_i.pts$) are stored as the training dataset. On the other hand, test data ($Test\_j.ref$ and $Test\_j.pts$) are collected at 36 locations in the same map. Both the training path and test path are shown in **Fig. 7**.

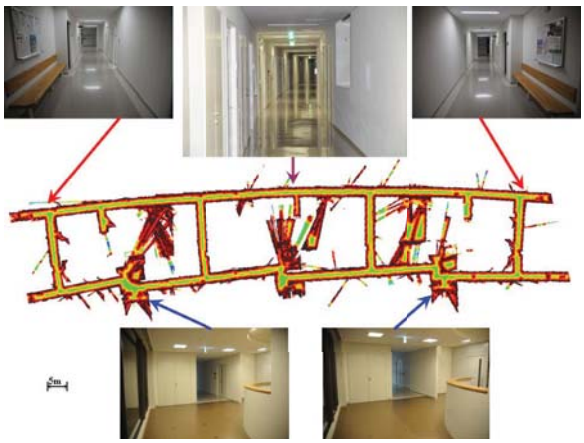

Fig. 6 Experimental areas.

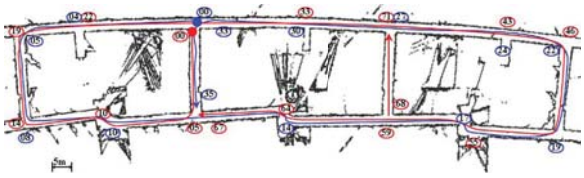

Fig. 7 Experimental paths, red line is the training path. blue line is the test path.

In Eq.(2), δ was set to be $2T$ where T is the average moving distance between the adjacent collecting positions of training dataset. Here T is set to be $3.6[m]$. With this value of δ, the number of candidates M (see Eq.(3)) is set to be 6. The particles converge to the correct location after the 5^{th} scanning position (shown as "04" in **Fig. 7**) in test path.

Table 1 shows the correctness of the initial localization within the 6 candidates estimated by BoF, i.e. in which rank the correct location is chosen within six candidates retrieved from the training dataset by the Kd-tree for each $Test\_j.ref$. The experimental results show that 31 locations in total are correctly estimated within 6 candidates for every $Test\_j.ref$. Especially in 19 positions, the positions of the robot are correctly estimated as the first candidate. In two positions, the second candidate and the fourth candidate are the actual locations, respectively. There are $36 - 31 = 5$ positions where the BoF can't initially estimate robot's location correctly. So the final accuracy is $31/36 \approx 86.1\%$. Note that although proper initial locations are not obtained at 5 positions from the BoF, the correct position is estimated by the automatic ICP after 5^{th} location thanks to the particle filter.

Particle filter excludes false estimation and finds true robot's location. The efficiency of particle filter is verified by automatic ICP. As mentioned in 21), four non-coplanar true pairs of matching 3D points are enough for calculation of a rigid transformation. By setting the parameters of voting algorithm (see 21) for more details), all of right candidate correspondences can be correctly aligned by automatic ICP. Since after the location "04" (i.e. the 5^th location in test path), all false candidates are excluded by particle filter. Therefore, correct corresponding $Train\_i.pts$ and $Test\_j.pts$ are found, and robot's location are all correctly estimated in remaining positions. **Figure 8** shows the comparison between the localization of particle filter and final precise localization by Automatic ICP. Among the red points, before location "04", particles don't converge to correct locations. These locations are excluded by Auto-ICP and corresponding red points are not shown in **Fig. 8**. **Figure 9** shows an example of alignment between $train\_10.pts$ $test\_10.pts$ and 2D features of reflectance images. Their locations are shown in **Fig. 7**.

Table 1 Results from searching in BoF.

No.	1st	2nd	3rd	4th	5th	6th	total
Correct localization	19	1	5	1	2	3	31

7. Conclusion

We proposed and demonstrated a two-step strategy combined with particle filter for global localization of a mobile robot in environments with strong perceptual aliasing. Besides the combination of appearance-based global localization and map-based global localization which improve the performance of correct position estimation, particle filter is used for further excluding false initial localization in appearance-based localization. The reflectance image, which is obtained as a byproduct of range sensing and is independent of the variation of the illumination condition, is used for appearance-based global localization in the first step. Precise map-based global localization by ICP is applied using 3D local maps, which are selected by the first step. The effectiveness of the proposed technique is demonstrated through experiments in an indoor image sequence with strong perceptual aliasing.

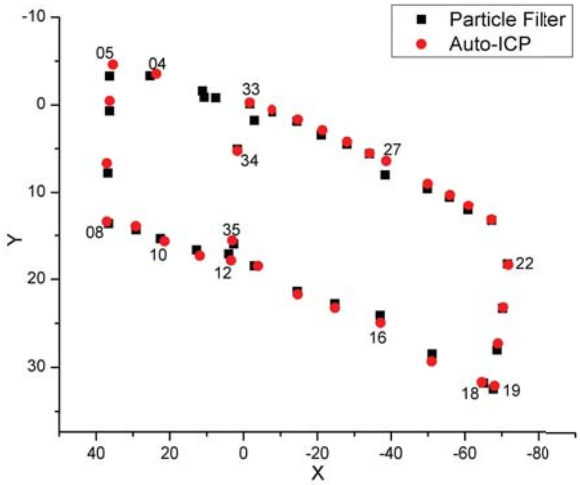

Fig. 8 Comparison between the particle filter location and alignment of automatic ICP.

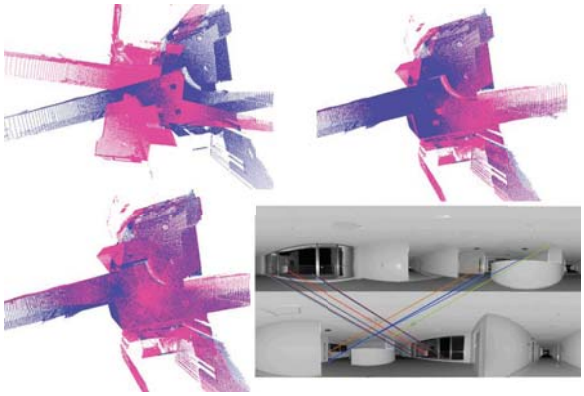

Fig. 9 From right to left, then top to bottom: Original 3D points; Roughly aligned 3D points by voting algorithm and RANSAC; Precisely aligned 3D points by ICP; Matched features in reflectance images.

Acknowledgement
The present study was supported in part by a Grant-in-Aid for Scientific Research (B) (23360115).

A.1. Laser-based environmental modeling by multiple mobile robots

For map-based global localization, an environmental map must be created and provided beforehand. For precise 3D mapping of the environment around a robot, we have proposed an efficient and precise system called CPS-SLAM[5], which can construct a rather accurate large-scale 3D map by means of a laser range finder and multiple robots based on technology used for geographical surveying. This technique is used as the basis of the urban search and rescue (USAR) robot[6].

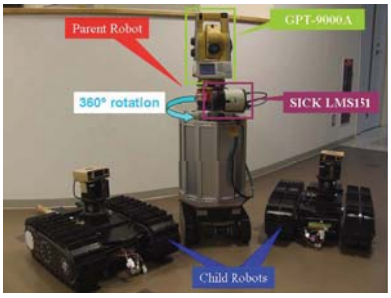

Fig. A.1 Three-dimensional modeling robots, CPS-VI.

Table A.1 Laser range finder (SICK LMS151).

Measuring range	50[m]
Field of view	270[○]
Precision	±30[mm]
Angular resolution	0.25[○]

Figure A.1 shows the sixth CPS-SLAM model, called CPS-VI. This system consists of one parent robot and two child robots. The parent robot is equipped with a highly precise laser range finder (GPT-9000A, TOPCON LTD), a 2D laser range finder (SICK LMS151), and a three-axis attitude sensor. The two child robots are equipped with corner cubes. The GPT-9000A and corner cubes are used cooperatively for self-positioning, as shown in **Fig. A.2**. The LMS151 (**Table A.1**) placed on a rotating table acquires two-dimensional slit-like range data, which are vertical to the ground. This sensor can capture reflectance data at the same time. Therefore, by rotating the table around the vertical axis for 360 ° while scanning with a 2D laser range finder, 3D range data and a 2D reflectance image are acquired. The number of pixels on a reflectance image is exactly the same as the number of 3D points in the range data, i.e., there exists a one-to-one mapping relationship between 2D pixels of the reflectance image and 3D points of the local 3D map.

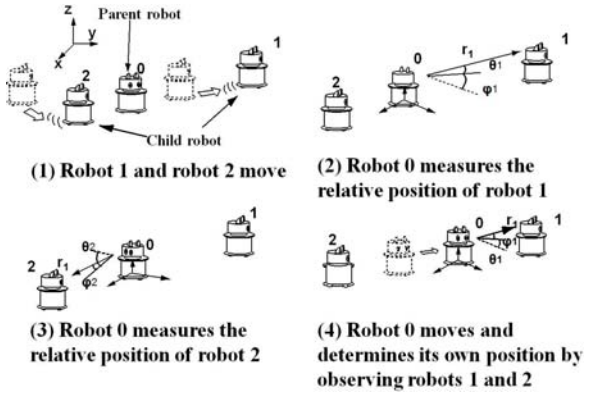

Fig. A.2 Cooperative positioning system (CPS).

References

1) D. Filliat, J.-A. Meyer, "Map-based navigation in mobile robots: I. A review of localization strategies", *Cognitive Systems Research*, vol. 4, no. 4, pp. 243-282, 2003.
2) A. Angeli, D. Filliat, S. Doncieux, and J.A. Meyer, "A Fast and Incremental Method for Loop-Closure Detection Using Bags of Visual Words", *IEEE Transactions on Robotics*, vol. 24, no.5, pp. 1027-1037, 2008.
3) M. Cummins, P. Newman, "FAB-MAP: Probabilistic Localization and Mapping in the Space of Appearance", *International Journal of Robotics Research*, vol. 27, no. 6, pp. 647-665, 2008.
4) Y. Hara, H. Kawata, A. Ohya and S. Yuta, "Mobile Robot Localization and Mapping by Scan Matching using Laser Reflection Intensity of the SOKUIKI Sensor", *IEEE Industrial Electronics, IECON*, pp. 3503-3508, 2006.
5) R. Kurazume, S. Hirose, "An Experimental Study of a Cooperative Positioning System", *Journal of Autonomous Robots*, vol. 8, no. 1, pp. 43-52, 2000.
6) M. Guarnieri, R. Kurazume, H. Masuda, "HELIOS system: A team of tracked robots for special urban search and rescue operations", *IEEE/RSJ International Conference on Intelligent Robots and Systems, IROS*, pp. 2795-2800, 2009.
7) S. Thrun, S. Thayer, W. Whittaker et al, "Autonomous exploration and mapping of abandoned mines: Software architecture of an autonomous robotic system", *IEEE Robotics and Automation Magazine*, vol. 11, no. 4, pp. 79-91, 2004.
8) J. Levinson, S. Thrun, "Robust vehicle localization in urban environments using probabilistic maps", in *Proc. IEEE International Conference on Robotics and Automation*, pp. 4372-4378, 2010.
9) P. J. Besl, N. D. McKay, "A method for registration of 3-D shapes", *IEEE Transactions on Pattern Analysis and Machine Intelligence*, vol. 14, no. 2, pp. 239-256, 1992.
10) C. S. Chen, Y. P. Hung, "RANSAC-Based DARCES: A new approach to fast automatic registration of partially overlapping range images" , *IEEE Transactions on Pattern Analysis and Machine Intelligence*, vol. 21, no. 11, pp. 1229-1234, 1999.

11) F. Bonin-Font, A. Ortiz and G. Oliver, "Visual Navigation for Mobile Robots: A Survey", *Journal of Intelligent and Robotic Systems: Theory and Applications*, vol. 53, no. 3, pp.263-296, 2008.
12) S. Thrun, D. Fox, W. Bugard and F. Dellaert, "Robust Monte Carlo localization for mobile robots", *Artificial Intelligence*, vol. 128, pp. 99-141, 2001.
13) Y. Matsumoto, M. Inaba, H. Inoue, "Visual navigation using view-sequenced route representation", in *Proc. IEEE International Conference on Robotics and Automation*, vol. 1, pp. 83-88, 1996.
14) T. Ohno, A. Ohya, S. Yuta, "Autonomous navigation for mobile robots referring pre-recorded image sequence", *IEEE International Conference on Intelligent Robots and Systems*, vol. 2, pp. 672-679, 1996.
15) E. Menegatti, M. Zoccarato, E. Pagello, H. Ishiguro, "Image-based Monte Carlo localisation with omnidirectional images", *Robotics and Autonomous Systems*, vol. 48, no. 1, pp. 17-30, 2004.
16) J. Wolf, W. Burgard, H. Burkhardt, "Robust vision-based localization for mobile robots using an image retrieval system based on invariant features", *IEEE International Conference on Robotics and Automation*, vol. 1, pp. 359-365, 2002.
17) H. Andreasson, A. Treptow, T. Duckett, "Self-localization in non-stationary environments using omnidirectional vision", *Robotics and Autonomous Systems*, vol. 55, no. 7, pp. 541-551, 2007.
18) A.C. Murillo, J.J. Guerrero, C. Sagüés, "SURF features for efficient robot localization with omnidirectional images", *IEEE International Conference on Robotics and Automation*, pp. 3901-3907, 2007.
19) P. Zingaretti, E. Frontoni, "Vision and sonar sensor fusion for mobile robot localization in aliased environments", *IEEE/ASME International Conference on Mechatronic and Embedded Systems and Applications*, pp. 116-121, 2006.
20) C. Valgren, A.J. Lilienthal, "SIFT, SURF & seasons: Appearance-based long-term localization in outdoor environments", *Robotics and Autonomous Systems*, vol. 58, no. 2, pp. 149-156, 2010.
21) D. X. Zhang, R. kurazume, Y. Iwashita, T. Hasegawa, "Appearance and map-based global localization using laser reflectivity", in *Proc. IEEE International Conference on Robotics and Biomimetics*, pp.1010-1016, 2011.